



LAMINAR FREE AND FORCED MAGNETOCONVECTION THROUGH AN OCTAGONAL CHANNEL WITH A HEAT GENERATING CIRCULAR CYLINDER

Rehena Nasrin* and M. A. Alim

Department of Mathematics, Bangladesh University of Engineering and Technology, Dhaka-1000, Bangladesh.

*Email: rehena@math.buet.ac.bd

Abstract:

In this paper, hydromagnetic flow and thermal behaviors of fluid on free and forced convection inside an octagonal vertical channel are investigated. The channel consists of a centered heat generating hollow solid circular cylinder. The vertical and inclined walls of the octagon are insulated perfectly. The input and output opening are situated at the bottom and top surface respectively. The octagon is filled with electrically conducting fluid. The integral forms of the governing equations are solved numerically using Galerkin's Weighted Residual Finite Element method. Computational domains are divided into finite numbers of body fitted control volumes with collocated variable arrangement. Results are presented in the form of average Nusselt number (Nu) and maximum temperature (θ_{max}) of the fluid for a selected range of magnetic parameter Hartmann number Ha (0 - 50). Streamlines and isothermal lines are also displayed for three different values (0.1, 1 and 10) of convection parameter (Ri) and for a fluid having magnetic field. The results indicate that the highest Nu and θ_{max} are found for the absence of Ha in all convection regions.

Keywords: Heat generation, circular cylinder, octagonal channel, free and forced magnetoconvection, finite element method.

NOMENCLATURE

B_0	magnetic field strength ($Wb\ m^{-2}$)	ΔT	dimensional temperature difference (K)
C_p	specific heat at constant pressure ($JKg^{-1}K^{-1}$)	u, v	velocity components (ms^{-1})
d	dimensional size of the conducting body (m)	U, V	non-dimensional velocity components
D	non-dimensional size of the solid body	x, y	Cartesian coordinates (m)
g	acceleration due to gravity (ms^{-2})	X, Y	non-dimensional Cartesian coordinates
h	convective heat transfer coefficient ($Wm^{-2}K^{-1}$)	Greek symbols	
Ha	Hartmann number	α	thermal diffusivity (m^2s^{-1})
K	solid-fluid thermal conductivity ratio	β	thermal expansion coefficient (K^{-1})
k	thermal conductivity ($Wm^{-1}K^{-1}$)	θ	non-dimensional temperature
L	length of the cavity (m)	μ	dynamic viscosity of the fluid ($Kg\ m^{-1}s^{-1}$)
Nu	Nusselt number	ν	kinematic viscosity of the fluid (m^2s^{-1})
p	dimensional pressure (Nm^{-2})	ρ	density of the fluid ($Kg\ m^{-3}$)
P	non-dimensional pressure	σ	electrical conductivity of the fluid ($\Omega^{-1}m^{-1}$)
Pr	Prandtl number	Subscripts	
q	generated heat per unit volume (Wm^{-2})	f	fluid
Q	heat generating parameter	h	heated wavy wall
Re	Reynolds number	i	less heated lid
Ri	Richardson number	max	maximum
T	dimensional temperature of fluid (K)	s	solid

1. Introduction

Mixed convection in channels is of vast interest of the phenomenon in many technological processes, such as the design of solar collectors, thermal design of buildings, air conditioning and the cooling of electronic circuit boards. In recent years, alteration of heat transfer in channels due to introduction of obstacles, partitions and fins attached to the wall(s) has received sustained attention. A literature review on the subject shows that many authors have considered mixed convection in vented enclosures with obstacles, partitions and fins, thereby altering the convection flow phenomenon. Actual enclosures in practice are often found to have different shapes rather than rectangular ones. Some examples of non-rectangular channels include various channels of constructions, panels of electronic equipment and solar energy collectors etc. Several geometrical configurations, more or less complex, have been examined under theoretical, numerical or experimental approaches. A combined free and forced convection flow of an electrically conducting fluid in a channel in the presence of magnetic field is of special technical significance because of its frequent occurrence in many industrial applications such as geothermal reservoirs, cooling of nuclear reactors, thermal insulations and petroleum reservoirs. These types of problems also arise in electronic packages, microelectronic devices during their operations.

Saha et al. (2010) performed natural convection heat transfer within octagonal enclosure. Their results showed that the effect of Ra on the convection heat transfer phenomenon inside the enclosure was significant for all values of Pr studied (0.71-50). It was also found that, Pr influenced natural convection inside the enclosure at high Ra ($Ra > 10^4$). Very recently Rahman et al. (2011) developed the magnetic field effect on mixed convective flow in a horizontal channel with a bottom heated open enclosure. Their results indicated that the magnetic field strongly affected the flow phenomenon and temperature field inside the cavity whereas this effect was less significant in the channel. Previously, similar problem for the case of assisting forced flow configuration was tested experimentally by Manca et al. (2006) and based on the flow visualization results. They pointed out that for $Re = 1000$, there were two nearly distinct fluid motions: a parallel forced flow in the channel and a recirculation flow inside the cavity and for $Re = 100$, the effect of a stronger buoyancy determined a penetration of thermal plume from the heated plate wall into the upper channel. Bhoite et al. (2005) studied numerically the problem of mixed convection flow and heat transfer in a shallow enclosure with a series of block-like heat generating component for a range of Reynolds and Grashof numbers and block-to-fluid thermal conductivity ratios. Results showed that higher Reynolds number created a recirculation region of increasing strength at the core region and the effect of buoyancy became insignificant beyond a Reynolds number of typically 600, and the thermal conductivity ratio had a negligible effect on the velocity fields. Brown and Lai (2005) conducted a horizontal channel with an open cavity and obtained correlations for combined heat and mass transfer which covered the entire convection regime from natural, mixed to forced convection.

Unsteady mixed convection in a horizontal channel containing heated blocks on its lower wall was performed numerically by Najam et al. (2003). Also, Singh and Sharif (2003) extended their previous work by considering six placement configurations of the inlet and exit ports of a differentially heated rectangular enclosure whereas the earlier work was limited only two different configurations of inlet and exit port. Conjugate mixed convection arising from protruding heat generating ribs attached to substrates forming channel walls is numerically analyzed by Madhusudhana and Narasimham (2007). The obtained outcome was that the natural convection induced mass flow rate in mixed convection was correlated in terms of the Grashof and Reynolds numbers. In pure natural convection it varied as 0.44 power of Grashof number. The maximum temperature was correlated in terms of pure natural convection and forced convection inlet velocity asymptotes and the heat transferred to the working fluid via substrate heat conduction was found to account for 41–47% of the heat removal from the ribs. Tsay et al. (2003) rigorously investigated the thermal and hydrodynamic interactions among the surface-mounted heated blocks and baffles in a duct flow mixed convection. They focused particularly on the effects of the height of baffle, distance between the heated blocks, baffle and number of baffles on the flow structure and heat transfer characteristics for the system at various Re and Gr/Re^2 .

Rahman et al. (2010) studied numerically the effect of Prandtl number on hydromagnetic mixed convection in a double-lid driven cavity with a heat-generating obstacle. They found that the flow and temperature field were strongly depend on the above stated parameter for the values considered. The variation of the average Nusselt number, the average temperature of the fluid and the temperature at the body centre for various Richardson number had been presented. Very recently, Parvin and Nasrin (2012) investigated Reynolds and Prandtl number effects on mixed convection in an octagonal channel. Couple effects of hydromagnetic and Joule heating on natural convective flow in an obstructed cavity was rigorously analyzed by Rehena Nasrin (2011) where the heat transfer rate grew up with rising Prandtl number while it devalued for increasing magnetic and Joule heating parameters.

On the basis of the literature review, it appears that no work was reported on mixed convection in an octagonal channel with heat generating circular block. The present study addresses the effects of imposed magnetic field and Richardson number on the thermal and flow fields for such geometry. The numerical computation covers a wide range of Hartmann number ($0 \leq Ha \leq 50$) and Richardson number ($0.1 \leq Ri \leq 10$).

2. Problem Formulation

The geometry of the problem herein investigated is depicted in Fig. 1. The system consists of an octagonal channel with sides of length L , within which a heat generating hollow circular body with outer diameter d is centered. The hollow circular body has a thermal conductivity of k_s and generates uniform heat q per unit volume. All solid walls of the octagon are considered to be adiabatic. It is assumed that the incoming flow has a uniform velocity, v_i and temperature, T_i . The inlet opening is located at the bottom, whereas the outlet opening is at the top of the octagon. A magnetic field of strength B_0 is acting in a transverse direction normal to the vertical walls of the octagon.

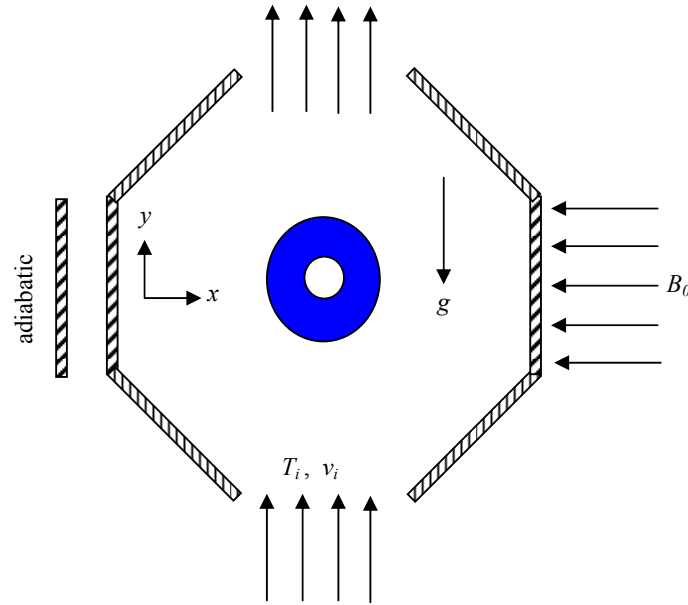


Fig. 1: Physical model of the octagonal channel

3. Mathematical Formulation

A two-dimensional, steady, laminar, incompressible, mixed convection flow is considered within the channel and the fluid properties are assumed to be constant. The radiation effects are taken as negligible. The dimensional equations describing the flow under Boussinesq approximation used by Nasrin and Parvin (2012) are as follows:

$$u \frac{\partial u}{\partial x} + v \frac{\partial u}{\partial y} = -\frac{1}{\rho} \frac{\partial p}{\partial x} + \nu \left(\frac{\partial^2 u}{\partial x^2} + \frac{\partial^2 u}{\partial y^2} \right) \tag{1}$$

$$u \frac{\partial v}{\partial x} + v \frac{\partial v}{\partial y} = -\frac{1}{\rho} \frac{\partial p}{\partial y} + \nu \left(\frac{\partial^2 v}{\partial x^2} + \frac{\partial^2 v}{\partial y^2} \right) + g\beta(T - T_c) - \frac{\sigma B_0^2 \nu}{\rho} \tag{2}$$

$$u \frac{\partial T}{\partial x} + v \frac{\partial T}{\partial y} = \frac{k_f}{\rho c_p} \left(\frac{\partial^2 T}{\partial x^2} + \frac{\partial^2 T}{\partial y^2} \right) \tag{3}$$

$$\tag{4}$$

For hollow cylinder the energy equation is

$$\frac{k_s}{\rho c_p} \left(\frac{\partial^2 T_s}{\partial x^2} + \frac{\partial^2 T_s}{\partial y^2} \right) + q = 0 \tag{5}$$

The boundary conditions for the present problem can be written as follows:

at the inlet: $u = 0, v = v_i, T = T_i$

at the outlet: convective boundary condition $p = 0$

at the cylinder boundary: $u = 0, v = 0, T_s = T_h$

at the walls of the octagon: $u = 0, v = 0, \frac{\partial T}{\partial n} = 0$

at the fluid-solid interface: $\left(\frac{\partial T}{\partial n} \right)_{fluid} = \frac{k_s}{k_f} \left(\frac{\partial T_s}{\partial n} \right)_{solid}$

The rate of heat transfer is computed at the heat generating cylinder and is expressed in terms of the local Nusselt number \overline{Nu} as $\overline{Nu} = \frac{hL}{k_s} = -\frac{\partial T_s}{\partial n} L$

where n is the non-dimensional distances either along x or y direction acting normal to the surface and k_f and k_s are the thermal conductivity of the fluids and the solid respectively.

The above equations are non-dimensionalized by using the following dimensionless quantities

$$X = \frac{x}{L}, Y = \frac{y}{L}, D = \frac{d}{L}, U = \frac{u}{v_i}, V = \frac{v}{v_i}, P = \frac{p}{\rho v_i^2}, \theta = \frac{(T - T_i)}{(T_h - T_i)}, \theta_s = \frac{(T_s - T_i)}{(T_h - T_i)}$$

Where X and Y are the coordinates varying along horizontal and vertical directions respectively, U and V are the velocity components in the X and Y directions respectively, θ is the dimensionless temperature and P is the dimensionless pressure.

Then the governing equations take the non-dimensional form given below

$$\frac{\partial U}{\partial X} + \frac{\partial V}{\partial Y} = 0 \tag{6}$$

$$U \frac{\partial U}{\partial X} + V \frac{\partial U}{\partial Y} = -\frac{\partial P}{\partial X} + \frac{1}{Re} \left(\frac{\partial^2 U}{\partial X^2} + \frac{\partial^2 U}{\partial Y^2} \right) \tag{7}$$

$$U \frac{\partial V}{\partial X} + V \frac{\partial V}{\partial Y} = -\frac{\partial P}{\partial Y} + \frac{1}{Re} \left(\frac{\partial^2 V}{\partial X^2} + \frac{\partial^2 V}{\partial Y^2} \right) + Ri \theta - \frac{Ha^2}{Re} V \tag{8}$$

$$U \frac{\partial \theta}{\partial X} + V \frac{\partial \theta}{\partial Y} = \frac{1}{Re Pr} \left(\frac{\partial^2 \theta}{\partial X^2} + \frac{\partial^2 \theta}{\partial Y^2} \right) \tag{9}$$

For heat generating obstacle the energy equation is

$$\frac{K}{Re Pr} \left(\frac{\partial^2 \theta_s}{\partial X^2} + \frac{\partial^2 \theta_s}{\partial Y^2} \right) + Q = 0 \tag{10}$$

where $Re = \frac{v_i L}{\nu}$, $Pr = \frac{\nu}{\alpha}$, $Ri = \frac{g \beta \Delta T L}{v_i^2}$ and $Q = \frac{qL^2}{k_s \Delta T}$ are Reynolds number, Prandtl number, Richardson number and heat generating parameter respectively. Also magnetic parameter (Ha) is defined as $Ha^2 = \sigma B_0^2 L^2 / \mu$,

The boundary conditions for the present problem are specified as follows:

at the inlet: $U = 0, V = 1, \theta = 0$

at the outlet: convective boundary condition $P = 0$

at cylinder boundary: $U = 0, V = 0, \theta_s = 1$

at the walls of the octagon: $U = 0, V = 0, \frac{\partial \theta}{\partial N} = 0$

at the fluid-solid interface: $\left(\frac{\partial \theta}{\partial N}\right)_{fluid} = K \left(\frac{\partial \theta_s}{\partial N}\right)_{solid}$

where K is the dimensionless ratio of the thermal conductivity (k_s / k_f) .

The local Nusselt number at the hollow circular tube is $\overline{Nu} = -\frac{\partial \theta_s}{\partial N} L$

The normal temperature gradient can be written as $\frac{\partial \theta_s}{\partial N} = \sqrt{\left(\frac{\partial \theta_s}{\partial X}\right)^2 + \left(\frac{\partial \theta_s}{\partial Y}\right)^2}$

The average Nusselt number at the heat generating body may be expressed as: $Nu = -\frac{1}{L_s} \int_0^{L_s} \frac{\partial \theta_s}{\partial N} dS$

where N, L_s and S are the non-dimensional distances either X or Y direction acting normal to the surface, arc length and coordinate along the circular surface respectively.

4. Finite Element Simulation

The momentum and energy balance equations are the combinations of mixed elliptic-parabolic system of partial differential equations that have been solved by using the Galerkin weighted residual finite element technique. The continuity equation has been used as a constraint due to mass conservation. The basic unknowns for the above differential equations are the velocity components U, V the temperature, θ and the pressure, P . The six node triangular element is used in this work for the development of the finite element equations. All six nodes are associated with velocities as well as temperature; only the corner nodes are associated with pressure. This means that a lower order polynomial is chosen for pressure and which is satisfied through continuity equation. The velocity component and the temperature distributions and linear interpolation for the pressure distribution according to their highest derivative orders in the differential equations (7) - (10) as given in Nasrin (2011)

$$U(X, Y) = N_\beta U_\beta, V(X, Y) = N_\beta V_\beta, \theta(X, Y) = N_\beta \theta_\beta, \theta_s(X, Y) = N_\beta \theta_{s_\beta}, P(X, Y) = H_\lambda P_\lambda, \text{ where } \beta = 1, 2, \dots, 6; \lambda = 1, 2, 3.$$

Substituting the element velocity component distributions, the temperature distribution and the pressure distribution from equations (7) - (10) the finite element equations can be written in the form

$$K_{\alpha\beta\gamma^x} U_\beta U_\gamma + K_{\alpha\beta\gamma^y} V_\beta V_\gamma + M_{\alpha\mu^x} P_\mu + \frac{1}{Re} \left(S_{\alpha\beta^{xx}} + S_{\alpha\beta^{yy}} \right) U_\beta = Q_{\alpha^u} \tag{11}$$

$$K_{\alpha\beta\gamma^x} U_\beta V_\gamma + K_{\alpha\beta\gamma^y} V_\beta V_\gamma + M_{\alpha\mu^y} P_\mu + \frac{1}{Re} \left(S_{\alpha\beta^{xx}} + S_{\alpha\beta^{yy}} \right) V_\beta - Ri K_{\alpha\beta} \theta_\beta + \frac{Ha^2}{Re} K_{\alpha\beta} V_\beta = Q_{\alpha^v} \tag{12}$$

$$K_{\alpha\beta\gamma^x} U_\beta \theta_\gamma + K_{\alpha\beta\gamma^y} V_\beta \theta_\gamma + \frac{1}{Re Pr} \left(S_{\alpha\beta^{xx}} + S_{\alpha\beta^{yy}} \right) \theta_\beta = Q_{\alpha^\theta} \tag{13}$$

$$\frac{K}{Re Pr} \left(S_{\alpha\beta^{xx}} + S_{\alpha\beta^{yy}} \right) \theta_\beta + Q = Q_{\alpha^{\theta_s}} \tag{14}$$

where the coefficients in element matrices are in the form of the integrals over the element area and along the element edges S_o and S_w as

$$\begin{aligned}
 K_{\alpha\beta^x} &= \int_A N_\alpha N_{\beta,x} dA, & K_{\alpha\beta^y} &= \int_A N_\alpha N_{\beta,y} dA, & K_{\alpha\beta\gamma^x} &= \int_A N_\alpha N_\beta N_{\gamma,x} dA, & K_{\alpha\beta\gamma^y} &= \int_A N_\alpha N_\beta N_{\gamma,y} dA, \\
 K_{\alpha\beta} &= \int_A N_\alpha N_\beta dA, & S_{\alpha\beta^{xx}} &= \int_A N_{\alpha,x} N_{\beta,x} dA, & S_{\alpha\beta^{yy}} &= \int_A N_{\alpha,y} N_{\beta,y} dA, & M_{\alpha\mu^x} &= \int_A H_\alpha H_{\mu,x} dA, \\
 M_{\alpha\mu^y} &= \int_A H_\alpha H_{\mu,y} dA, & Q_{\alpha^u} &= \int_{S_0} N_\alpha S_x dS_0, & Q_{\alpha^v} &= \int_{S_0} N_\alpha S_y dS_0, & Q_{\alpha^\theta} &= \int_{S_w} N_\alpha q_{1w} dS_w, \\
 Q_{\alpha^\theta_s} &= \int_{S_w} N_\alpha q_{2w} dS_w.
 \end{aligned}$$

The set of non-linear algebraic equations (11) - (14) are solved using reduced integration technique of Reddy (1999), Zeinkiewicz et al. (1971) and Newton-Raphson method of Roy and Basak (2005).

4.1 Grid Refinement Test

In order to determine the proper grid size for this study, a grid independence test is conducted with five types of mesh for $Pr = 1.73$, $Re = 10$, $Ri = 1$, $Q = 5$, $K = 5$, $Ha = 10$ and $D = 0.3$. The extreme values of Nu and θ_{max} are used as a sensitivity measure of the accuracy of the solution and are selected as the monitoring variables. Considering both the accuracy of numerical values and computational time, the present calculations are performed with 40295 nodes and 10936 elements grid system.

Table 1: Grid Sensitivity Check at $Pr = 1.73$, $Re = 10$, $Ri = 1$, $Q = 5$, $K = 5$, $Ha = 10$ and $D = 0.3$

Nodes (elements)	7224 (4816)	12982 (5784)	26538 (8992)	40295 (10936)	80524 (18080)
Nu	2.312753	2.026821	1.715743	1.415496	1.415495
θ_{max}	1.232832	1.091826	1.069835	1.0218254	1.0218253
Time (s)	226.265	292.594	388.157	421.328	627.375

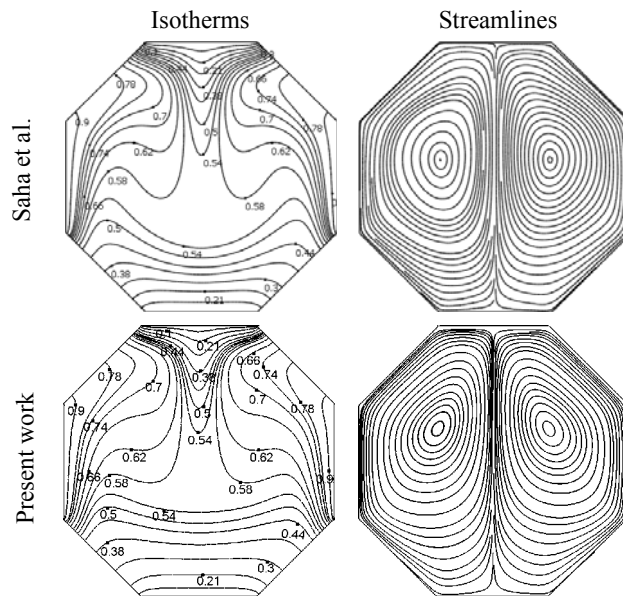


Fig. 2: Comparison between present numerical code and Saha et al. (2010) using $Ra = 10^4$ and $Pr = 0.71$

4.2 Code Validation

A description of the code and its validation are available in Nasrin and Parvin (2011) and are not repeated here. The existing code in Nasrin and Parvin (2011) has been modified for the current problem.

4.3 Comparison

The model comparison is an essential part of a mathematical investigation. Hence, the outcome of the present numerical code is benchmarked against the numerical result of Saha et al. (2010) which was reported for natural convection flow and heat transfer within octagonal enclosure. The comparison is conducted while employing the dimensionless parameters $Ra = 10^4$ and $Pr = 0.71$. Present result for both the streamlines and isotherms is shown in Fig. 2, which is an outstanding agreement with those of Saha et al. (2010). This justification boosts the assurance in this numerical code to carry on with the above stated objective of the existing investigation

4.4 Mesh Generation

In finite element method, the mesh generation is the technique to subdivide a domain into a set of sub-domains, called finite elements, control volume etc. The discrete locations are defined by the numerical grid, at which the variables are to be calculated. It is basically a discrete representation of the geometric domain on which the problem is to be solved. The computational domains with irregular geometries by a collection of finite elements make the method a valuable practical tool for the solution of boundary value problems arising in various fields of engineering. Fig. 3 displays the finite element mesh of the present physical domain.

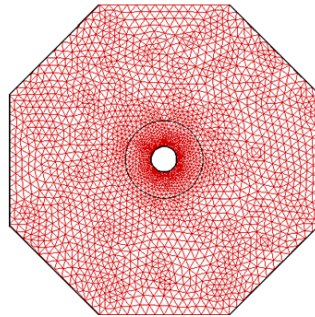


Fig. 3: Mesh structure for vertical channel with a heat generating pipe

5. Results and Discussion

The mixed convection phenomenon inside a two sided open octagon having a heat-generating hollow circular block is influenced by different controlling parameters such as Hartmann number Ha , Richardson number Ri , Prandtl number Pr , solid fluid thermal conductivity ratio K , heat generating parameter Q and diameter D of the circular body. Analysis of the results is made through obtained streamlines, isotherms, average Nusselt number and maximum temperature of the fluid for two significant parameters, Ha and Ri . The ranges are varied as $0 \leq Ha \leq 50$ and $0.1 \leq Ri \leq 10$, while the other parameters K , Re , D , Pr and Q are kept fixed at 5, 10, 0.3, 1.73 and 5 respectively.

Fig. 4 (a) – (b) provide the information about the influence of Ha at the forced convection dominated region ($Ri = 0.1$) on isotherms as well as streamlines. Thermal boundary layer thickness reduces as Ha increases and the isothermal lines become denser at the adjacent area of the heat source. The flow with the absence of magnetic field ($Ha = 0$) creates a couple of tiny recirculation regions near the heat generating hollow cylinder as shown in Fig. 4 (b). These spinning regions disappear sequentially and the streamlines cover all the area of the octagon by varying Ha .

The influence of magnetic parameter at the mixed convection region ($Ri = 1$) on temperature and flow fields is depicted in Fig. 5 (a) – (b). The isothermal lines are more concentrated near the heat-generating obstacle. Also, the bend in isothermal lines appears due to the free and forced convective current inside the channel. Consequently, the flow pattern changes radically due to the deviation of Ha . For escalating values of Ha , the eddy present in the flow field diminishes by size. This is because, the magnetic field acts against the flow and reduces the fluid velocity.

Thermal current and flow activities are offered in Fig. 6 (a) – (b) with different Hartmann number and purely free convection effect ($Ri = 10$). For higher Ha , the isothermal lines take an onion shape from the circular body to exit port. This is due to confining the thermal boundary layer for the effect of higher magnetic field. The lines

become more concentrated from the forced convection dominant region to free convection dominant regime for a particular Ha . On the other hand, size of spinning cells in the velocity field becomes larger due to buoyancy force for increasing Ri ($= 10$) with compared to the previous Figs. 4(b) and 5(b). In addition, the flow field bifurcates near the circular body.

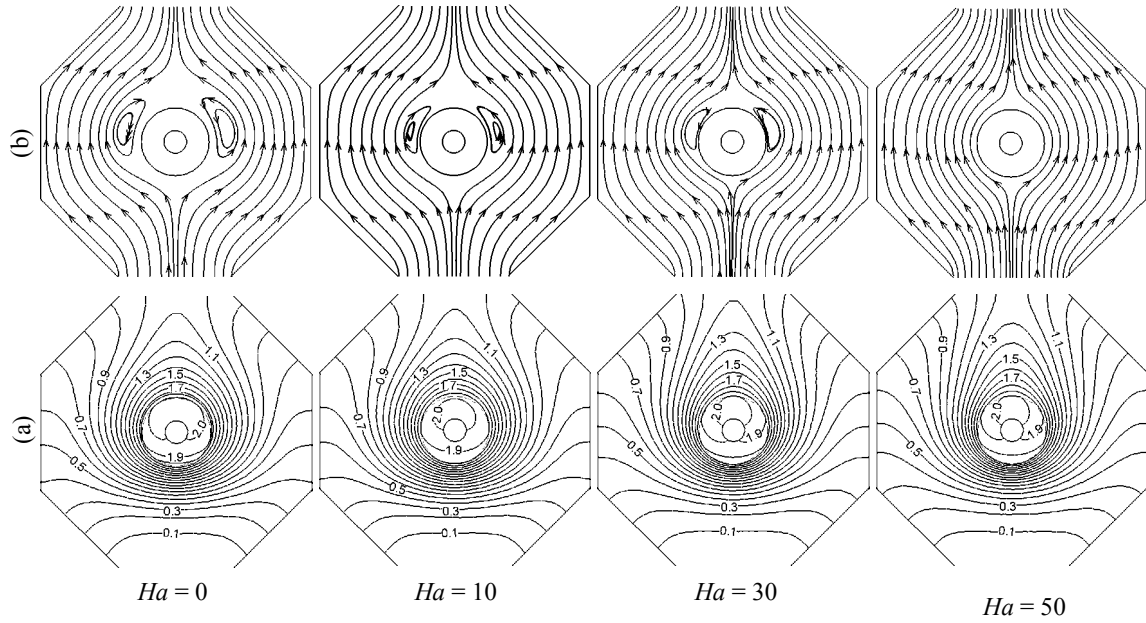


Fig. 4: Effect of Hartmann number at $Ri = 0.1$ on (a) Isotherms and (b) Streamlines

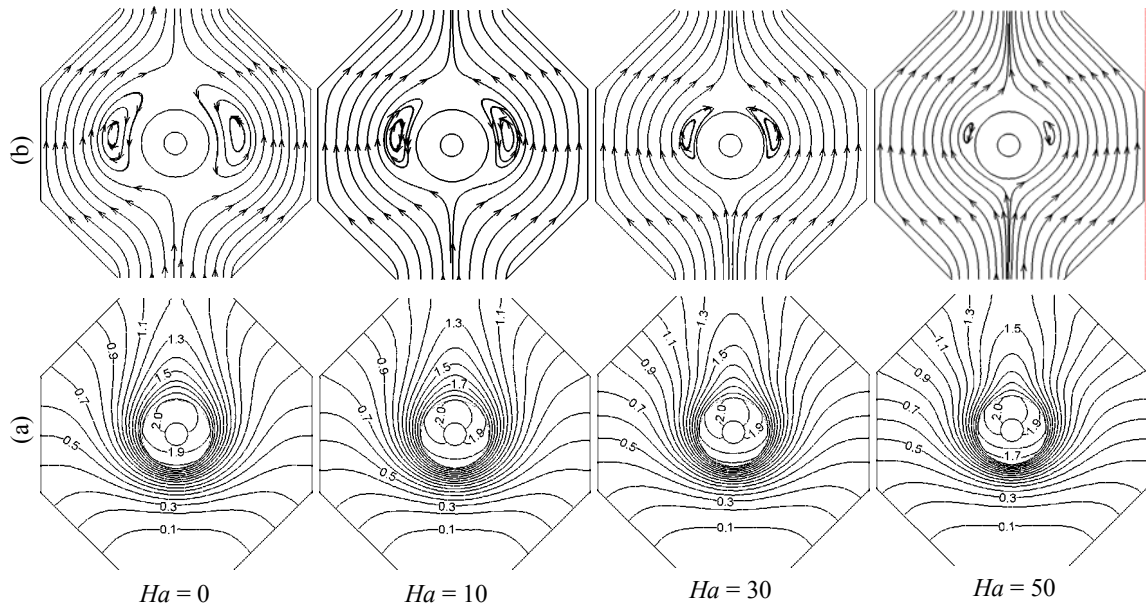


Fig. 5: Effect of Hartmann number at $Ri = 1$ on (a) Isotherms and (b) Streamlines

The variations of the average Nusselt number (Nu) at the heated surface and the maximum temperature of the fluid (θ_{max}) for different magnetic parameter with Richardson numbers have been presented in Fig. 7. It is clearly seen from the figure that for a particular value of Ri , the heat transfer rate and maximum temperature of fluid are the lowest for the largest Hartmann number $Ha = 50$. For the reason that the fluid with the absence of magnetic field is capable to carry more heat away from the heat source and dissipated through the out flow

opening. Moreover, Nu remains invariant for higher values of Hartmann number and it rises very unhurriedly for the lowest Ha due to rising Ri . On the other hand, at $Ha = 0$, θ_{max} devalues sharply in the forced convection dominated region ($Ri \leq 1$) and then it remains constant with mounting Ri . In addition, for the remaining Ha , it is decreases slowly for varying Ri .

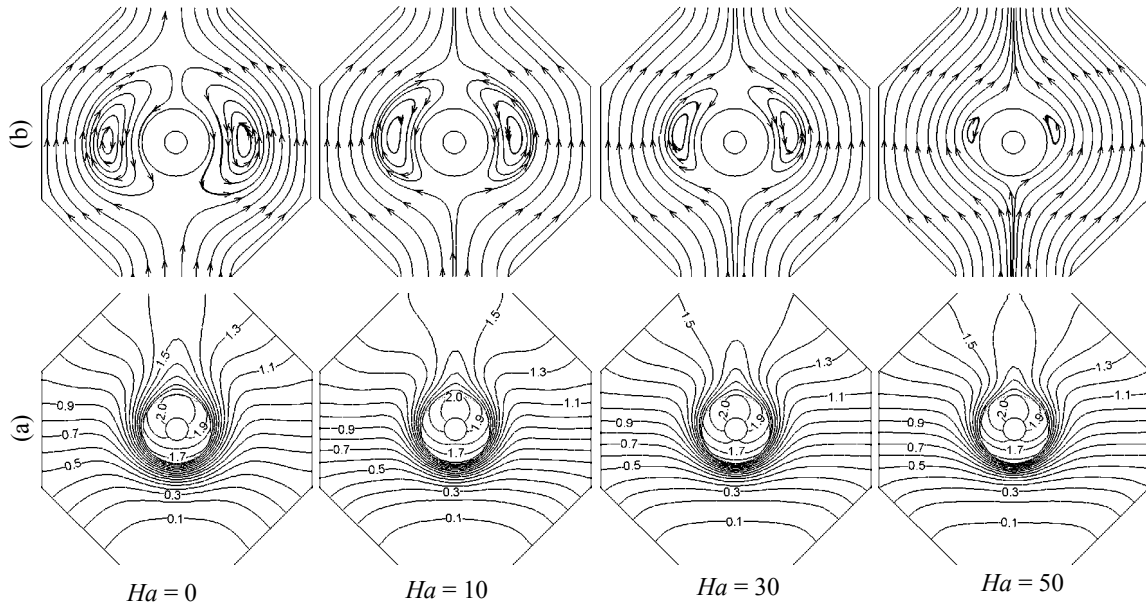


Fig. 6: Effect of Hartmann number at $Ri = 10$ on (a) Isotherms and (b) Streamlines

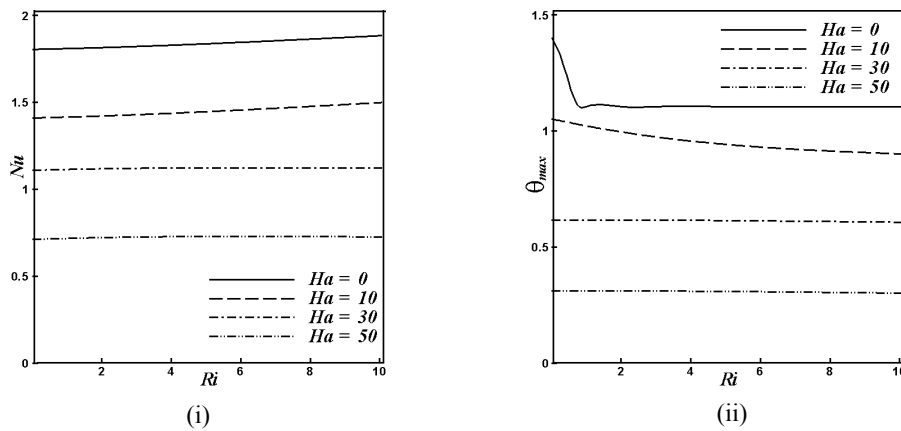


Fig. 7: Effect of Hartmann number on (i) average Nusselt number and (ii) maximum temperature of the fluid

6. Conclusion

A computational study is performed to investigate the hydromagnetic mixed convection in an octagonal channel with a heat-generating horizontal circular body. Results are obtained for wide ranges of Hartmann number Ha and Richardson number Ri . The following outcomes may be written from the present investigation:

- The influence of convection parameter Ri on isotherms and streamlines are remarkable for the different values of magnetic parameter.
- Thermal layer near the heated surface become thin and concentrated. Vortices created by inertia and buoyancy force in the streamlines lessen for the hindrance of the imposed magnetic field.

- Escalating the Ha devalues the average Nusselt number at the heated surface as well as the maximum temperature of the fluid.

References

- Bhoite, M. T., Narasimham, G. S. V. L. and Murthy, M. V. K (2005): Mixed convection in a shallow enclosure with a series of heat generating components, International Journal of Thermal Sciences, Vol. 44, No. 2, pp.121-135. <http://dx.doi.org/10.1016/j.ijthermalsci.2004.07.003>.
- Brown, N. M. and Lai, F.C. (2005): Correlations for combined heat and mass transfer from an open cavity in a horizontal channel, International Communication in Heat and Mass Transfer, Vol. 32, No. 8, pp. 1000–1008.
- Manca, O., Nardini, S. and Vafai, K. (2006): Experimental investigation of mixed convection in a channel with an Open Cavity, Experimental Heat Transfer, Vol. 19, pp. 53–68.
- Najam, M., Amahmid, A., Hasnaoui, M. and Alami, M. E. (2003): Unsteady mixed convection in a horizontal channel with rectangular blocks periodically distributed on its lower wall, International Journal of Heat and Fluid Flow, Vol. 24, pp. 726-735.
- Nasrin, R. (2011): Finite element simulation of hydromagnetic convective flow in an obstructed cavity, International Communications in Heat and Mass Transfer, Vol. 38, No. 5, pp. 625-632. <http://dx.doi.org/10.1016/j.icheatmasstransfer.2011.02.005>.
- Nasrin, R. (2011): Rayleigh and Prandtl number effects on free and forced magnetoconvection in a lid driven enclosure with wavy bottom wall, International Journal of Energy and Technology, Vol. 3, No. 23, pp. 1-8.
- Nasrin, R. and Parvin, S. (2011): Hydromagnetic effect on mixed convection in a lid-driven cavity with sinusoidal corrugated bottom surface, International Communications in Heat and Mass Transfer, Vol. 38, No. 6, pp. 781-789. <http://dx.doi.org/10.1016/j.icheatmasstransfer.2011.03.002>.
- Nasrin, R. and Parvin, S. (2012): Flow behavior for combined convection in a vertical channel controlled by a heat-generating tube, International Journal of Energy & Technology, Vol. 4, No. 1, pp. 1-7.
- Parvin, S. and Nasrin, R. (2012): Effects of Reynolds and Prandtl number on mixed convection in an octagonal channel with a heat-generating hollow cylinder, Journal of Scientific Research, Vol.4, No.2, pp. 337-348.
- Rahman, M. M., Nasrin, R. and Billah, M. M. (2010): Effect of Prandtl number on hydromagnetic mixed convection in a double-lid driven cavity with a heat-generating obstacle, Engineering e-Transaction, Vol. 5, No. 2, pp. 90-96.
- Rahman, M. M., Parvin, S., Saidur, R. and Rahim, N.A. (2011): Magneto hydrodynamic mixed convection in a horizontal channel with an open cavity, International Communications in Heat and Mass Transfer, Vol. 38, pp. 184–193. <http://dx.doi.org/10.1016/j.icheatmasstransfer.2010.12.005>.
- Rao, G. M. and Narasimham, G. S. V .L. (2007): Laminar conjugate mixed convection in a vertical channel with heat generating components, International Journal of Heat and Mass Transfer, Vol. 50, No. 17-18, pp. 3561-3574.
- Reddy, J. N. (1993): An Introduction to Finite Element Analysis, McGraw-Hill, New-York.
- Roy, S. and Basak, T. (2005): Finite element analysis of natural convection flows in a square cavity with non uniformly heated wall(s), International Journal of Engineering Sciences, Vol. 43, pp. 668-680.
- Saha, G., Saha, S., Hasan, M. N. and Islam, M .Q. (2010): Natural convection heat transfer within octagonal enclosure, IJE Transactions A: Basics, Vol. 23, No. 1, pp. 1-10.
- Singh, S. and Sharif, M.A.R. (2003): Mixed convection cooling of a rectangular cavity with inlet and exit openings on differentially heated side walls, Numerical Heat Transfer, Part A, Vol. 44, pp. 233–253.
- Tsay, Y. L., Cheng, J. C. and Chang, T. S. (2003): Enhancement of heat transfer from surface-mounted block heat sources in a duct with baffles, Numerical Heat Transfer, Part A, Vol. 43, pp. 827-841.
- Zeinkiewicz, O. C., Taylor, R. L. and Too, J. M. (1971): Reduced integration technique in general analysis of plates and shells, International Journal for Numerical Methods in Engineering, Vol. 3, pp. 275-290. <http://dx.doi.org/10.1002/nme.1620030211>.